# *Diagnostic Methods for Investigating the Ignition Process in Large Gas Engines*

*Dr. Gerhard Pirker, Prof. Andreas Wimmer, Dr. Georg Meyer, Dr. Constantin Kiesling – LEC GmbH; Andreas Nickl, Anton Tilz – Technische Universität Graz*

## Abstract

Numerous studies have shown that spark ignited gas engines currently play an important role in decentralized energy supply concepts and will continue to do so in the future. To meet stringent emission limits while maintaining high engine efficiency, there is a trend towards higher mean effective pressures and ultra-lean highly turbulent combustion concepts. Under these severe ignition conditions, it is increasingly challenging to limit cycle-to-cycle combustion variability to acceptable levels. Given the central role of the ignition process, this publication provides a report on fundamental research on all aspects of spark ignition as a prerequisite to understanding the relevant sub-processes of the electronic ignition system, electric arc and flame kernel development and subsequently improving engine performance.

The fundamental research on spark ignition is addressed following the LEC Development Methodology (LDM), which approaches problems using specifically tailored experimental investigations and simulations of fundamental processes. An optically accessible arc test rig allows investigation of electric arc behavior in an inert atmosphere under engine-like pressures and flow velocities at the spark plug using high-speed imaging and sophisticated postprocessing algorithms. A rapid compression-expansion machine (RCEM) provides the opportunity to investigate the flame kernel development in the vicinity of the spark plug electrodes under engine-like and reactive (but nearly quiescent) conditions. In this case, optical accessibility in combination with high-speed imaging and sophisticated postprocessing algorithms also represents the key diagnostic method. Finally, investigations on a single cylinder research engine (SCE) equipped with ion current measurement technology are used to analyze the infant flame kernel development under real engine conditions, completing the picture of the ignition process and providing the basis for the validation and improvement of a spark ignition model.

The results illustrate how the results from the specific test rigs are transferable to the results obtained from the single cylinder engine measurements. It can be inferred that the cycle-to-cycle variability introduced by the electric arc behavior and along with it the variability of the spark energy contributes to the cycle-to-cycle variability observed in spark ignited internal combustion engines. Future research will apply the full range of the diagnostic methods presented here to gain further insight into the role of energy from spark ignition in heavy duty and large gas engines under lean conditions.


## 1. Introduction

Numerous studies have shown that spark ignited gas engines currently play an important role in decentralized energy supply concepts and will continue to do so in the future [1], [2]. While the diesel engine will still dominate the transportation (marine, rail) sector as the main source of propulsion, power generation applications will rely mainly upon gas engines [3], [4]. However, low emission gas engines may also be able to meet the very stringent emission requirements for marine applications especially in coastal regions [5], [6], [7], [8]. In recent years, the electrical efficiencies of gas engines have improved remarkably. Some have even reached values of over 50% with the lowest possible emissions, and the potential exists for a further improvement in efficiency [9]. The trend towards higher mean effective pressures and ultra-lean highly turbulent combustion concepts will continue. As a direct consequence, combustion stability has become an issue for robust engine operation [10], [11]. As the excess air ratio of the mixture and the mean effective pressures increase, the window for stable engine operation between misfire and knock becomes smaller, see Figure 1. Under these severe ignition conditions, limiting cycle-to-cycle variation to acceptable levels becomes increasingly challenging.

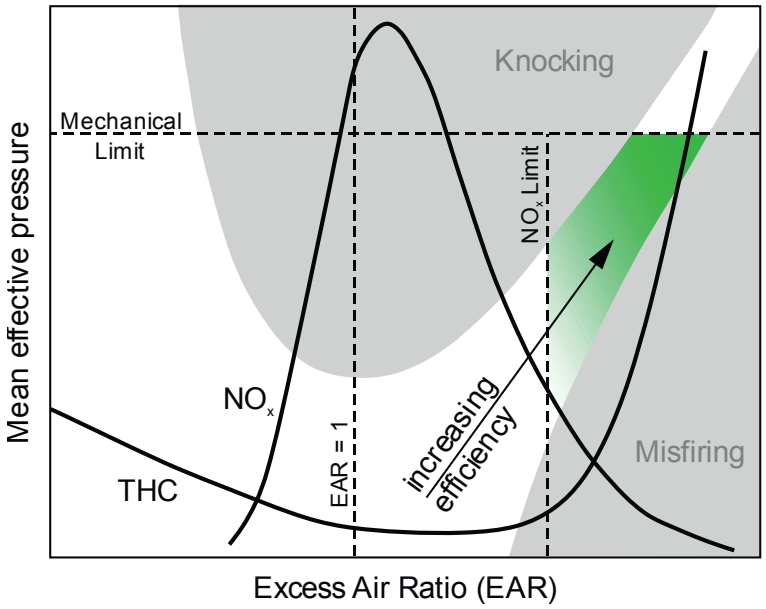


Figure 1: Ultra-lean mixtures and high mean effective pressures narrow down the window for stable engine operation [12].

Optimal performance of the ignition system is critical to supporting the development of the infant flame kernel into a stable flame front. Although research into alternative ignition concepts is being conducted, electronic ignition systems are the most widespread in engines worldwide. The development of high performance electronic ignition systems has contributed to the persistence of electronic ignition systems [13]. Therefore, it is expected that they will continue to dominate in gas engine operation.

A lean burn combustion concept requires optimal ignition system performance and influences the design and setup of the electronic ignition system. Figure 2 shows schematically the interaction of the ignition hardware, spark discharge, infant flame kernel development and global in-cylinder combustion associated with direct current electronic ignition technology. The purpose of the ignition system is to transfer electric energy stored in an ignition coil (inductive ignition system) or in a capacitor (capacitive discharge ignition systems) into the combustible mixture. The conversion of electrical to thermal energy is accomplished by the electric arc formed between the electrodes of the spark plug after breakdown, which is achieved via a high-voltage pulse. Local flow field and thermodynamic conditions, e.g., pressure and mixture temperature at the spark plug, greatly influence the characteristics of the spark discharge and consequently determine the energy supplied

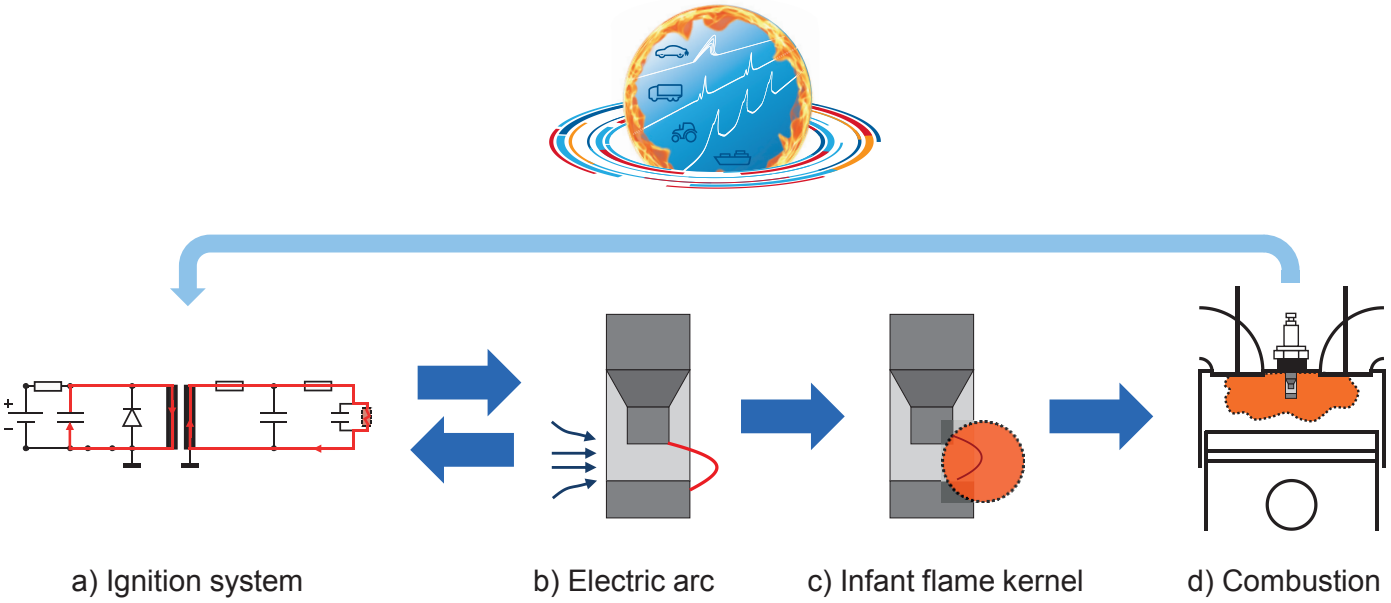


Figure 2: Interaction and influencing factors of ignition hardware, electric spark, infant flame kernel development and combustion in spark ignited engines.

by the ignition system that is available to initiate combustion. Strong flow fields have the ability to significantly stretch the electric arc. Since the electric arc serves as a conductor in the secondary circuit of the ignition system, in-cylinder conditions directly influence the discharge characteristics of the electronic ignition system. Once the supplied energy is sufficient to initiate the development of an infant flame kernel, the further energy supply helps to overcome heat losses due to turbulent flame quenching and the spark plug surface. If the process is successful, turbulent, stable flame propagation can develop. Global in-cylinder flow and turbulence intensities greatly influence and promote the combustion process and are crucial for thorough combustion in the cylinder.

Since the ignition process plays a key role in the overall combustion cycle and since it takes place under increasingly severe conditions, fundamental research into all aspects of spark ignition has to be pursued from both an experimental as well as from a modeling perspective. Optical diagnostic methods used to study the initial flame kernel development temporally and spatially significantly contribute to a better understanding of spark ignition. However, these techniques are difficult to apply in large gas engines due to the very limited access to the main combustion chamber and/or the prechamber.

In order to meet the challenges arising from these objectives, a clearly structured methodology is applied: LEC Development Methodology (LDM). LDM is based on the close interaction between simulation and experiments. In this publication, the methodology is specially tailored to the specific tasks – primarily experimental investigations of fundamental processes on special test rigs as well as a single cylinder research engine. Different test beds and diagnostic methods have been developed and used to study spark ignition in large gas engines. Although electrode wear and measures of mitigation to increase spark plug lifetimes are also important aspects of robust engine operation, they will not be addressed in this publication. Figure 3 provides an overview of the methodology that has been specially tailored to the tasks at hand.

Step 1 of the methodology involves modeling. A detailed spark ignition model has been developed and is currently being integrated into the CFD methodology [14]. This process rests upon highly sophisticated numerical methods that are applied to depict the detailed physical relationships. The model consists of several submodels that all require separate validation. In Step 2, specially tailored fundamental experiments that isolate certain aspects of the spark ignition process are conducted under very controlled experimental conditions. These investigations provide an extensive database for validating the submodels as well as valuable insight and fundamental knowledge into the ignition process. However, the complete model can only be validated with measurements on a real gas engine. The final Step 3 thus consists of model validation with measurements of a single cylinder research engine (SCE). The

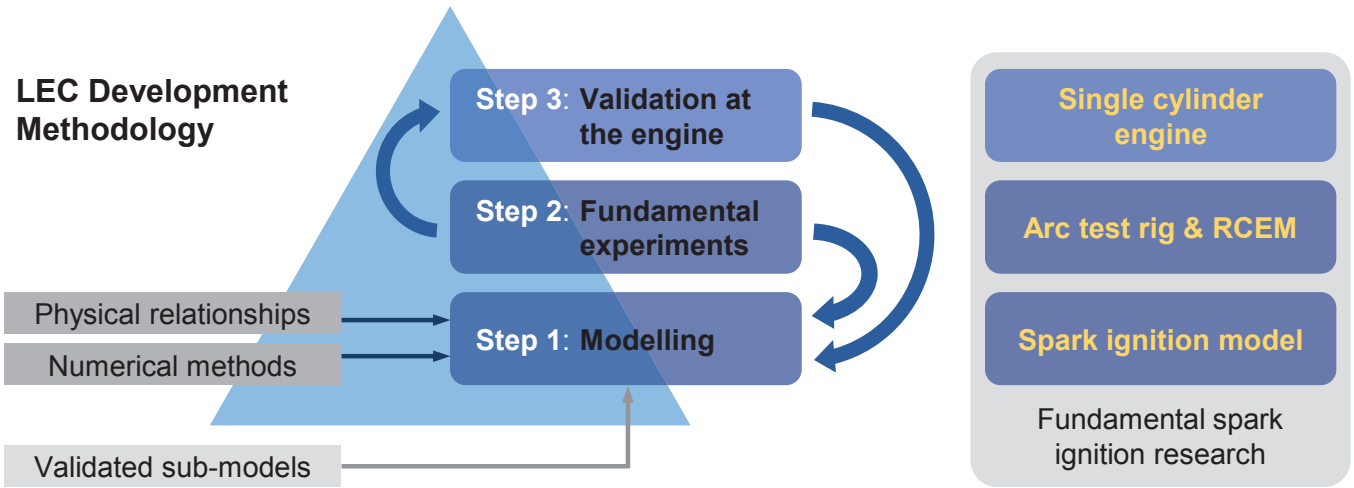


Figure 3: LEC Development Methodology (LDM).

knowledge obtained during model development and fundamental experiments provides critical input for the design of the SCE experiments. At the same time, results of both fundamental and SCE experiments are used to validate and to improve the modeling.

## 2. Diagnostic Methods

Based on the development methodology described above, the following test rigs have been designed to explore specific aspects of spark ignition by using diagnostic methods:

- The influence of flow and thermodynamic conditions on electric arc and the ignition system hardware and their mutual interaction are studied in the arc test rig described in section 2.1 using noncombustible gases. The focus is on the energy available for flame kernel generation and support which is transferred from the ignition system to the gas, see Figure 2 a) and b).
- The interaction of the infant flame kernel with spark plugs is studied in a rapid compression-expansion machine (RCEM) in section 2.2. This study focuses on heat loss to the spark plug electrodes, see Figure 2 c). Spark plug electrodes for gas engines exhibit significantly larger quenching surfaces at lower electrode gaps than automotive spark plugs, thereby meriting a more detailed investigation [15].
- The fundamental experiments focus on the surplus energy resulting from supplied spark energy and heat loss to electrodes. The scenario that contains all influences occurring in real engine operation, especially the influence of turbulence, can only be analyzed in a SCE, which is described in section 2.3. These measurements, therefore, focus on the complete functional chain, see Figure 2 a) - d), and require the development of special diagnostic methods to obtain information on early flame propagation.

The following subsections present the three diagnostic methods and explain the appropriate post-processing procedure for obtaining the relevant information with each method.

### 2.1 Arc test rig

The purpose of the arc test rig is to study spark behavior and its interaction with the ignition hardware under strong cross flow and turbulence levels at pressures in the range of 1 to 60 bar. This test rig enables detailed investigation of the spark energy input to the flowing gas as a key parameter for successful spark ignition. A non-reacting atmosphere is used throughout these experiments.

Figure 4 gives an overview of the test rig installation (left) and a detailed cross-sectional view of the test cell (right). The system provides controllable, stable and well-defined experimental conditions that are essential to interpreting the measurement results and generating a database for model validation.

The installation is designed as a closed circuit system that can be pressurized up to 60 bar. A hermetically sealed blower provides continuous gas flow, resulting in superficial velocities (volume-flow averaged velocities) of up to 30 m/s upstream of the spark plug. The temperature can be controlled by a heat exchanger. The key element is the test cell, which facilitates the installation of different spark plug variants and provides three windows for optical access (two windows opposite each other on each side, one window at the bottom of the cell). In addition, the orientation of the spark plug electrode can be adjusted in relation to the direction of the flow velocity. A mass flow meter and pressure and temperature sensors monitor stable operation. Prior to the measurement campaign, the flow field upstream of the spark plug was measured with CTA (constant temperature anemometry) so that the defined velocities at the spark plug were able to be assigned to the measured gas mass flows. To this end, an in-situ calibration procedure for high pressures was specifically developed at the LEC. The

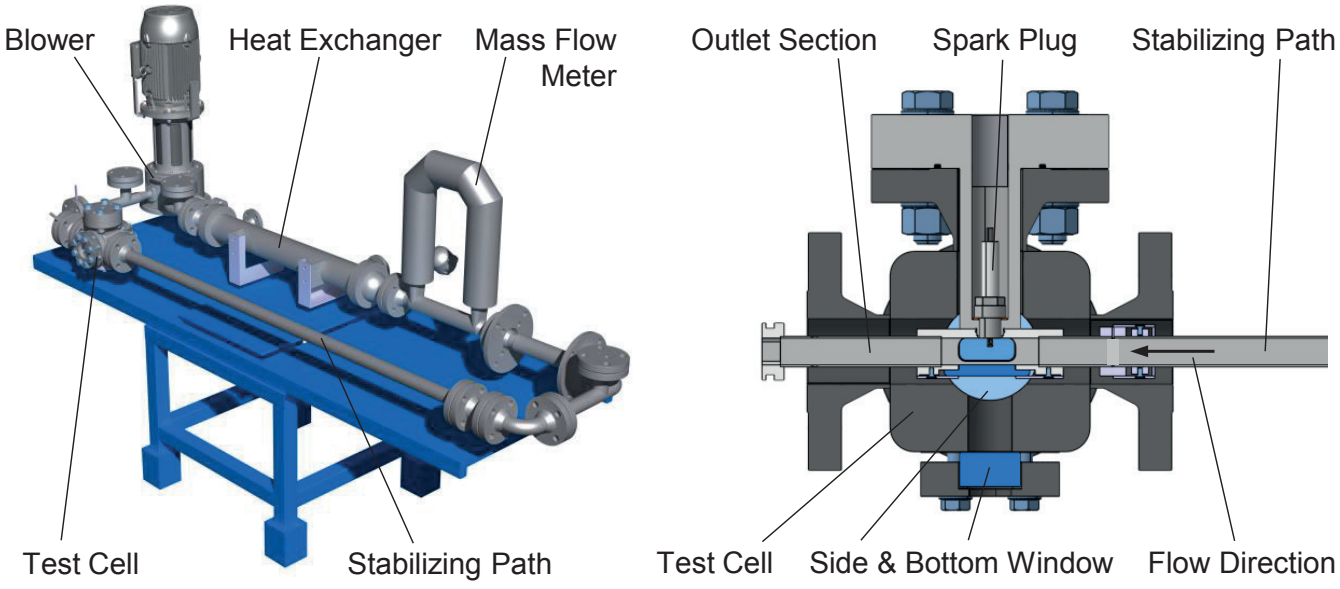


Figure 4: Arc test rig and cross-sectional view of test cell.

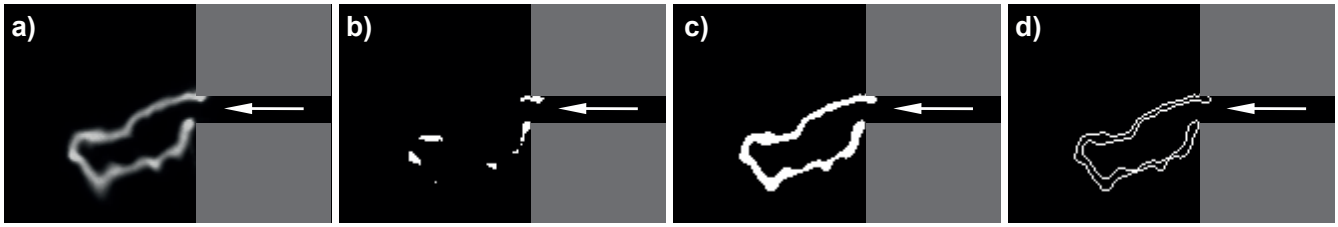


Figure 5: Steps of image processing to obtain the length of the electric arc.

behavior of the electrical arc is captured by a high-speed camera (Photron FASTCAM SA-X2) and the ignition system parameters (primary and secondary voltages and currents) are measured by an oscilloscope (Yokogawa DL850EV ScopeCorder Vehicle Edition). The high-speed camera and the oscilloscope measurements are synchronized by a trigger signal generated by the ignition system.

One important aspect of the diagnosis method is the automated quantitative evaluation of high-speed images. The length of the stretched arc is extracted from the high-speed images. The procedure developed at the LEC for image processing of electric arc recordings is shown in Figure 5.

The raw image is transformed into a binary black and white image using a threshold of 90%, see Figure 5 a) and b). After binarization is complete, the algorithm checks for disjunct areas of the white region(s). The threshold value is iteratively reduced until a continuous region is obtained for the first time, Figure 5 c). The interior is then removed, leaving behind only the outer contour of the formerly white region, Figure 5 d). The arc length is estimated by dividing the circumference of the outer contour by two. This measure is very good for elongated structures but poor for nearly spherical objects. A final check is performed to establish the degree of sphericity of the white region, which represents the electric arc. This algorithm proved to be more reliable and robust than other methods [16], which used a skeletization procedure.

## 2.2 Rapid compression-expansion machine (RCEM)

The rapid compression-expansion machine serves as test rig for the fundamental investigation of individual ignition and combustion processes in an engine-like environment with excellent optical accessibility and high flexibility in terms of piston stroke, compression ratio and composition of the gas mixture. In contrast to the experiments in the arc test rig, which used a non-reactive atmosphere and only investigated arc behavior, the investigations in the RCEM study the interaction of the infant flame kernel with the spark plug electrodes in detail.

Figure 6 provides a cross-sectional view of the machine with a hardware setup dedicated to the detailed analysis of spark ignition and combustion events with premixed gas-air mixtures. Similar to an internal combustion engine, the combustion chamber is surrounded by a cylinder head, cylinder liner and piston. The cylinder head includes a centrally located spark plug and several sensors but is otherwise flat (no intake/exhaust valves). The cylinder liner contains three lateral windows near the fire deck that provide optical access to the combustion chamber. The combustion chamber is also charged and drained through access bores in the liner. The piston (flat piston deck) is connected to a piston tube. A circular window in the piston deck in combination with a recess in the piston tube and a 45° mirror provide an additional optical access to the combustion chamber in the axial direction of the cylinder. A ballistic piston movement ("shot") is achieved by applying pressure to the end face of the piston tube with compressed air. A mass balancing piston between the compressed air and the piston tube is connected hydrodynamically to the piston tube and

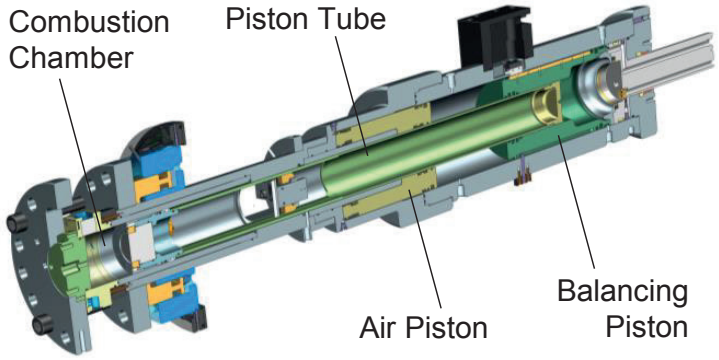


Figure 6: Cross-sectional view of the rapid compression-expansion machine.

moves in the opposite direction to compensate for the inertial forces during a shot. The pressurized air volume can be adjusted with an air piston and an adjustable external pressure reservoir (not shown in Figure 6). The bore diameter of the RCEM is set at 84 mm and the stroke can be adjusted to a maximum of 250 mm.

The same ignition system and measuring equipment (high-speed camera and oscilloscope, described above in section 2.1) were used for the measurements at the RCEM. In addition to recording the ignition system parameters, a piezoelectric pressure transducer captures the in-cylinder pressure trace during one shot. With the high-speed camera, different measurement techniques can be applied such as the schlieren technique and broadband imaging of light emission during ignition and combustion. Figure 7 provides an example of one sequence of images recorded for this study to illustrate the possibilities of investigating the flame kernel development.

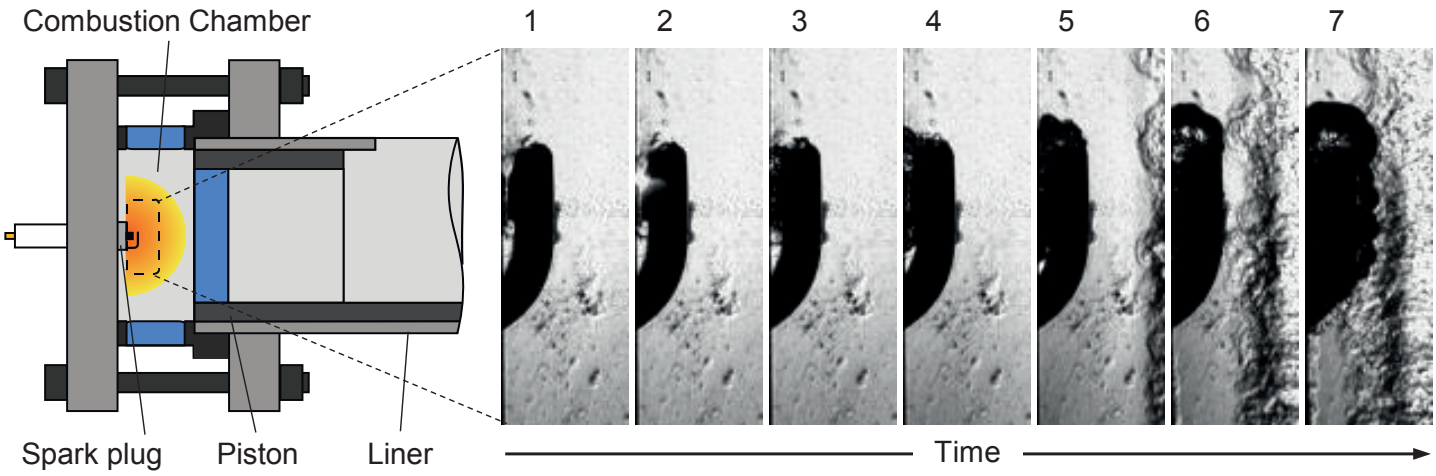


Figure 7: High-speed schlieren imaging of flame kernel development.

The left-hand side of Figure 7 shows a schematic view of the RCEM. The dashed rectangle within the combustion chamber indicates the area of the images visible on the right-hand side of the figure. The displayed sequence of images (time steps 1 to 7) was recorded through the lateral windows by schlieren imaging, which allows visualization of the flame front by means of density gradients in the premixed gas-air mixture [17]. In each image, the ground electrode of the spark plug can be identified by its dark, J-shaped display. After spark breakdown in time step number 2 (visible from the distinct light emission), the propagation of the flame within the gap of the spark plug can be seen. As time elapses, the flame area expands inside the gap and then propagates further into the combustion chamber.

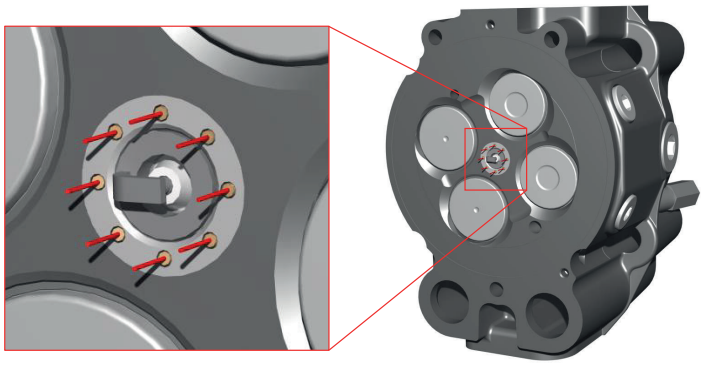

Figure 8: SCE cylinder head instrumented with ion current probes.

## 2.3 Single Cylinder Engine (SCE)

The next step of the diagnosis methodology employs a large high-speed four-stroke single cylinder engine with a displacement of approximately 4 dm³ in order to investigate ignition and infant flame kernel development under real engine conditions. To ensure reproducible testing conditions, the engine is supplied with conditioned charge air, burning gas, cooling water and lubricating oil on the test bed. The back pressure in the exhaust pipe is controlled by a flap to simulate the presence of a turbocharger.

For the present study, the engine was fitted with a cylinder head designed for open chamber combustion of a premixed gas-air mixture with a centrally located spark plug as the source of ignition, see Figure 8. Both the ignition system and the measurement technology for recording primary and secondary currents and voltages were the same as on the arc test rig. To supplement the standard technology for measuring the ignition system parameters and the in-cylinder pressure trace, eight ion current probes were fitted symmetrically around the spark plug at a radial distance of 10 mm from the spark plug thread axis. These probes detect the flame front arrival at their locations, thereby enabling detailed and robust analysis of

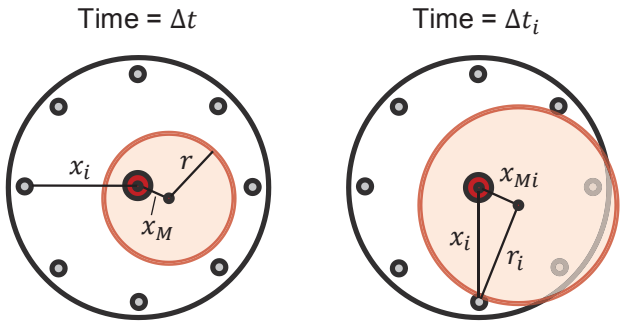


Figure 9: Computation of drift velocity and flame front velocity.

flame kernel development in the near vicinity of the spark plug [18], [19].

The ion current signals are sampled and recorded by the engine indication system. A special algorithm calculates the time of arrival of the flame front from the measurement signal of each individual ion current sensor. From the distance between the sensor and spark plug center and the ignition timing, a characteristic flame velocity can be computed and a polar diagram of flame velocities can be generated, yielding a two-dimensional visualization of the infant flame kernel development (described in detail in the following section). The definition of

a drift velocity and flame front velocity used as characteristic values is introduced in Figure 9 and explained below.

Assuming the infant flame kernel is spherical, the drift velocity denotes the mean velocity at which the center of the flame sphere is moving (cross flow effects) and the flame front velocity denotes the mean velocity at which the radius of the spherical flame ball increases. The red dot in Figure 9 indicate the spark plug position, x_i the ion current sensor position, x_M the position of the center of the flame ball. r denotes the radius of the flame ball. If the flame is detected at sensor i after the time Δt_i has elapsed since the start of ignition, then the values x_Mi and r_i are known for a given drift and flame front velocity. Each sensor provides a conditional equation for the unknowns, drift and flame front velocity. When more than three ion current sensors are used, this results in an overdetermined system of equations which is solved by quadratic error minimization.

## 3. Results and Discussion

The following section interprets the results obtained by applying the diagnostic methods presented in the previous section. The discussion focuses on selected illustrative results obtained with the different diagnostic methods for the arc test rig (section 2.1) and the SCE (section 2.3). Based on the RCEM results (section 2.2), it is assumed that the initial flame front propagation is approximately spherical. These results confirm the validity of the method for evaluating the SCE test bed results. The section concludes by describing current investigations at the LEC that make full use of the research methodology.

separate fundamental study, it is not discussed in this publication.

During each measurement, a sequence of 50 spark events was recorded at the given boundary conditions. Figure 10 shows a sequence of high speed images of three example arc events at the same experimental conditions (flow velocity 15 m/s, pressure 30 bar, temperature 70 °C). Since the flow direction in Figure 10 is from right to left, the time axis was also aligned in this direction. An image of the electrodes taken at longer exposure times was superimposed on each of the images of the electric arc for better visibility of the electrodes. This example used a special spark plug design with an electrode gap of 0.28 mm; the full measurement campaign included commercially available gas engine spark plugs as well. The three different spark events in Figure 10 labeled with a), b) and c) show that the stochastic distribution of breakdown locations over the electrode surface (visible at 25 µs) yields a markedly different evolution of the electric arc column. A closer look at the mechanism reveals three different causes for the observed variability of arc behavior:

- Breakdown location and associated differences in the local flow field seen by the electric arc as shown in Figure 10.
- Turbulent folding and wrinkling of the arc column as shown in Figure 10. It was found that wrinkling becomes more dominant at higher pressures and higher flow velocities.
- Restrikes or shortening of the arc column. The formation of a restrike can be observed in Figure 11. If electric arc segments approach each other, Figure 11 a), – also promoted by turbulent wrinkling – a restrike is possible, Figure 11 b). A thin conducting channel forms between the two segments, leading to a shortening of the electric arc column, Figure 11 c).

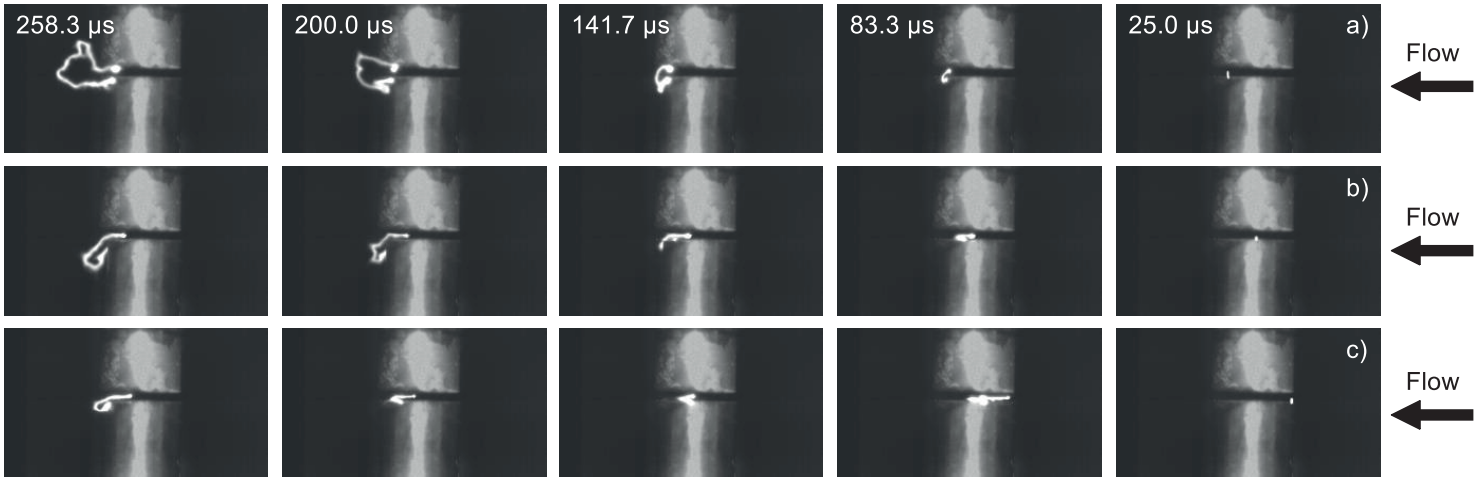


Figure 10: Influence of the location of spark breakdown on spark stretching.

The diagnostic methods applied to the fundamental investigations in the arc test rig provide a basis for discussion of the cycle-to-cycle variation observed in the electric arc behavior and the consequences for spark discharge even under very controlled experimental conditions. The influence of flow conditions and thermodynamic conditions (e.g., pressure) on arc behavior is equally important, yet since it is the subject of a

The cycle-to-cycle variation of the arc evolution has direct consequences on the spark energy input released by the electronic ignition system. Figure 12 shows the arc lengths and electric energy dissipated on the secondary side of the ignition system over time of 50 consecutive cycles. Note that the dissipated energy plotted in Figure 12 includes the energy consumed in the electric components as well. The thick solid line


Figure 11: Turbulent arc folding and the formation of a restrike.

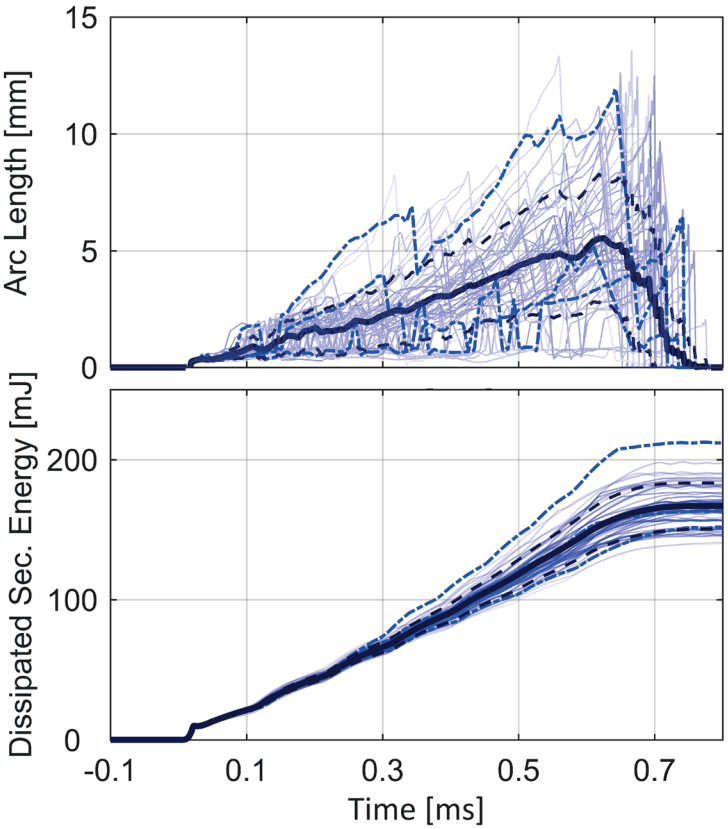


Figure 12: Temporal evolution of arc length and energy dissipated on the secondary side.

represents the average and the dashed lines the standard deviation. The dashed-dotted lines correspond to the three different arc sequences shown in Figure 10. Thus, the cycle-to-cycle variation of the electric arc directly translates into the cycle-to-cycle variation of the released spark energy.

The transferability of arc test rig results to the SCE measurements is shown in Figure 13. It can be inferred that the cycle-to-cycle variation introduced by the electric arc behavior and along with it the cycle-to-cycle variation of the spark energy contribute to the cycle-to-cycle variation observed in spark ignited internal combustion engines, see also the findings reported in [10]. However, other causes of cycle-to-cycle variation exist, e.g., the cycle-to-cycle variation of the global in-cylinder flow.

To study the influence of spark discharge characteristics on combustion performance in gas engines, measurements are performed on the SCE research engine described in section 2.3. In addition to in-cylinder pressure trace analysis, the ring of ion current sensors around the spark plug is used to investigate the infant flame kernel development, see section 2.3.

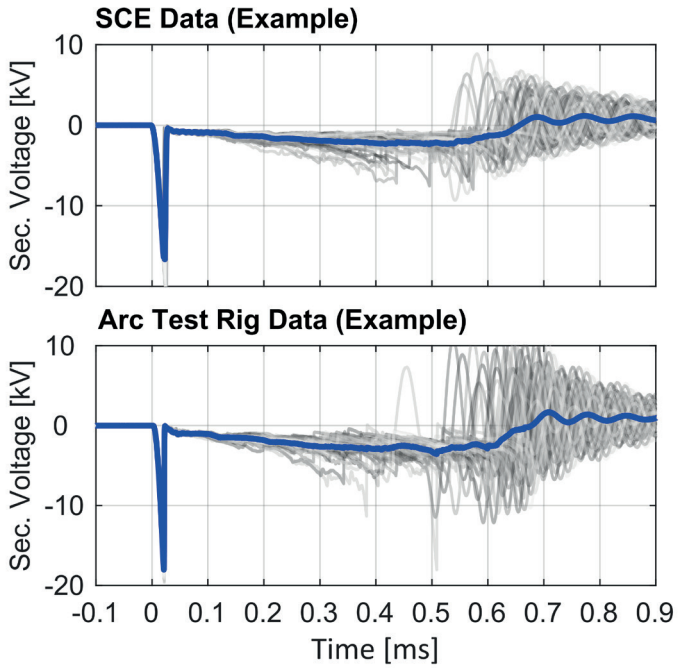


Figure 13: Transferability of arc test rig results to SCE measurements.

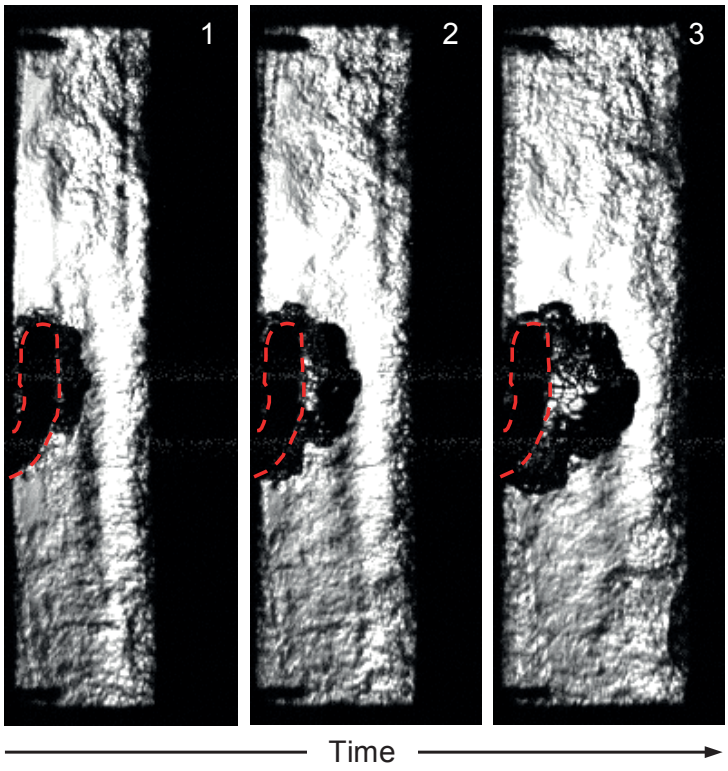


Figure 14: Schlieren imaging of early flame propagation.

Prior to the SCE measurements, optical investigations were carried out on the RCEM to obtain an impression of flame propagation in the area of the ion-current sensor ring. The shape of the flame was of particular interest. Figure 14 presents three schlieren images taken with boundary conditions

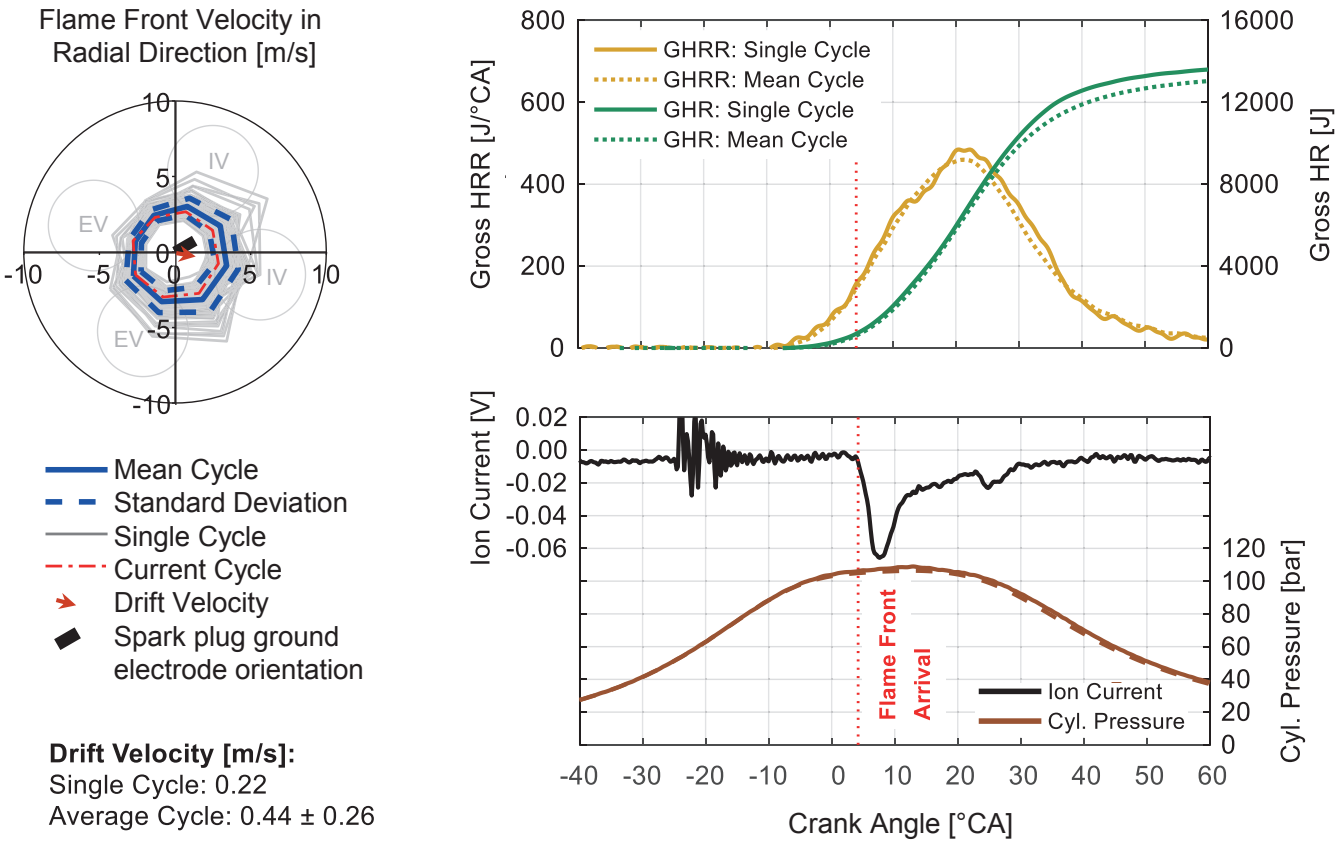


Figure 15: Post-processing combustion-related information on early flame kernel development in the research engine.

comparable to the SCE near Top Dead Center. Due to the flow conditions in the combustion chamber and the shape of the ground electrode of the spark plug, the flame front is not visible as a perfect sphere. Nevertheless, it can still be assumed that the flame propagates in a roughly spherical shape until it reaches the radius of the ion current probe ring. This conclusion is important for the SCE investigations and the computation of drift velocity and flame front velocity.

The result of the evaluation of the ion current sensor data is plotted in Figure 15 (left side) as a polar diagram for an operating point of the research engine running at full load and close to the lean limit. The light grey circles show the location of the inlet valves (IV) and exhaust valves (EV) with respect to the orientation of the unshielded J-gap spark plug used in the experiments. Also light grey are the 100 cycles recorded during one measurement, which provide an impression of the cycle-to-cycle variation, while the blue solid line shows the average and the dashed blue lines the standard deviation. One individual cycle depicted by the red dashed-dotted line in the upper left diagram of Figure 15 was selected as an example. The gross heat release (GHR) and the gross heat release rate (GHRR) as well as the the cylinder pressure of this single cycle are plotted in detail in the diagrams on the right-hand side of Figure 15. The ion current signal recorded for one of the sensors is also provided as an example in the lower diagram. The sudden drop in the ion current signal indicates the time of the flame front arrival. In addition to pressure sensor data, the ring of ion current sensors provides further insight into the spatial flame front development and the drift of the

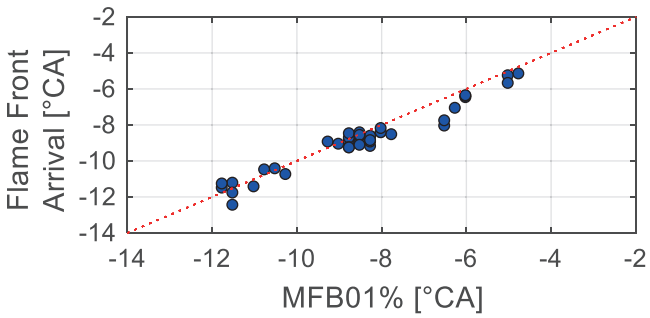


Figure 16: Correlation of pressure trace analysis and ion current data (SCE).

flame kernel from the spark plug. The applied methods – cycle resolved monitoring of the discharge characteristics of the ignition system and ion current sensing – permit the influence of the ignition system on flame kernel development to be studied methodically using different engine loads, combustion concepts (swirl, tumble) or fuel/air ratio and spark timing.

It is critical to check whether the information from post-processing of the ion current sensor signals correlates with the information extracted from the analysis of the heat release rate data. To this end, the mean time of flame front arrival obtained by the ion current measurements was compared to the MFB01% (1% mass fraction burned) taken from the heat release data

for different engine operation points; good agreement was obtained (Figure 16).

## 4. Summary and Outlook

Thorough knowledge of the processes during ignition and flame kernel development is a key prerequisite to ensuring stable and efficient ignition in spark-ignited combustion engines and serves as a basis for model development. This publication presented a comprehensive methodology of fundamental investigations which enables the understanding of the interaction of the ignition system with the ignition spark and the infant flame kernel development. The details of the applied test rigs, the diagnostic methods as well as the post-processing algorithms were discussed and compared.

High-speed imaging techniques were used to study the interaction between the spark behavior and the ignition hardware under strong cross flow and turbulence levels at inert conditions on a specially designed arc test rig. The stretched arc length, which turned out to be an important value for model validation, is evaluated quantitatively from the high-speed images with a highly sophisticated algorithm. Under reactive conditions in a rapid compression-expansion machine, the infant flame kernel and its interaction with the spark plug were optically investigated, leading to the assumption of a spherical flame front in the initial phase. Finally, ion current measurements in a single cylinder research engine were conducted to determine the influence of real engine conditions on the infant flame kernel, focusing on the complete functional chain and enabling comprehensive model validation.

The transferability of results from the arc test rig to the SCE measurements was demonstrated. The cycle-to-cycle variability of the arc behavior (and thus of the spark energy) contributes to the cycle-to-cycle variations observed in spark ignited internal combustion engines. The ion current signals correlate very well qualitatively with the MFB01% as shown by the heat release rate data extracted from the pressure sensor data.

Future research will apply the full range of diagnostic methods presented in this publication. By relating cycle-resolved information on burning velocities (SCE) to cycle-resolved information on spark energy, further insight will be gained into the role of energy on spark ignition in heavy duty and large gas engines under lean conditions. This work will be complemented by investigations in the RCEM of the influence of spark plug electrodes on the very early phase of spark ignition. Since gas engine spark plugs operate at significantly lower electrode gaps and are bulkier than automotive spark plugs, they merit an independent investigation.

## 5. Acknowledgement

The authors would like to acknowledge the financial support of the "COMET - Competence Centres for Excellent Technologies Programme" of the Austrian Federal Ministry for Transport, Innovation and Technology (BMVIT), the Austrian Federal Ministry of Science, Research and Economy (BMWFW) and the Provinces of Styria, Tyrol and Vienna for the K1-Centre LEC EvoLET. The COMET Programme is managed by the Austrian Research Promotion Agency (FFG). The authors would further like to thank GE Jenbacher GmbH & Co OG and Mr. Arno Gschirr from Hoerbiger Ventilwerke GmbH & Co. KG for the support and for providing equipment during the tests.

## Nomenclature

| | |
|---|---|
| CA | Crank angle |
| CFD | Computational fluid dynamics |
| EAR | Excess air ratio |
| EV | Exhaust valve |
| GHRR | Gross heat release rate |
| GHR | Gross heat release |
| IV | Inlet valve |
| LDM | LEC Development Methodology |
| LEC ter | Large Engines Competence Cen- |
| MFB01% | 1% mass fraction burned |
| NOx | Nitrogen oxides |
| RCEM chine | Rapid compression-expansion ma- |
| SCE | Single cylinder engine |
| THC | Total hydrocarbons |

## Literature

[1] E. Verdolini, F. Vona, and D. Popp, "Bridging the Gap: Do Fast Reacting Fossil Technologies Facilitate Renewable Energy Diffusion?," National Bureau of Economic Research, Working Paper 22454, Jul. 2016.

[2] W. Warnecke, J. Karanikas, B. Levell, C. Mesters, J. Schreckenberg, and J. Adolf, "Gas – A Bridging Technology for Future Mobility?," in: H. P. Lenz (Ed.), "34th International Vienna Motor Symposium 25. - 26. April 2013," (= Fortschritt-Berichte VDI Reihe 12, Nr. 764), Düsseldorf, 2013.

[3] OECD International Transport Forum, "ITF Transport Outlook 2017," Paris, 2017.

[4] G. Pirker and A. Wimmer, "Sustainable power generation with large gas engines," in: "Energy Conversion and Management," vol. 149, Oct. 2017, pp. 1048–1065.

[5] D. Hagen, C. Senghaas, M. Willmann and H. J. Koch, "Simplified L'Orange fuel injection system for Dual Fuel applications," in: H. Harndorf (Ed.), "Die Zukunft der Großmotoren IV, 4. Rostocker Großmotorentagung," Rostock, 2016, pp. 124–137.

[6] S. Pischinger, "Wie Gesetzgebungen und Kundenanforderungen Innovationen Beeinflussen," in: H. Harndorf (Ed.), "Die Zukunft der Großmotoren IV, 4. Rostocker Großmotorentagung," Rostock, 2016, pp. 1–19.

[7] B. Bucholz, "Saubere Großmotoren für die Zukunft - Herausforderung für die Forschung," in: H. Harndorf (Ed.), "Die Zukunft der Großmotoren III, 3. Rostocker Großmotorentagung," Rostock, 2014, pp. 1–14.

[8] J. Sell, "Marine Klassifikation von Gasmotoren - Beweggründe, Anforderungen, Herausforderungen," in: WTZ Roßlau GmbH (Hrsg.), "Proceedings, 9th Dessau Gas Engine Conference," Dessau, 2015, pp. 13–20.

[9] A. Wimmer, G. Pirker, M. Engelmayer, and E. Schnessl, "Gas engine versus Diesel engine: A comparison of efficiency," in: "MTZ industrial," vol. 1, no. 1, Nov. 2011, pp. 22–27.

[10] C. Poggiani, M. Battistoni, C. N. Grimaldi, and A. Magherini, "Experimental Characterization of a Multiple Spark Ignition System," in: "Energy Procedia," vol. 82, Dec. 2015, pp. 89–95.

[11] G. Meyer, A. Gschirr, T. Lindner-Silwester, and K. Stadlbauer, "Recent Advances in Modeling Modulated Capacitive High- Energy Ignition Systems and Application of the Findings in a New Generation of Ignition Systems," in: H. Eichlseder (Ed.), "14th Symposium The Working Process of the Internal Combustion Engine," Graz, 2013.

[12] R. Golloch and A. Wimmer, "Groß-Gasmotoren," in: G. Merker and R. Teichmann (Eds.), "Grundlagen Verbrennungsmotoren; Funktionsweise, Simulation, Messtechnik," 7th ed., Wiesbaden, 2014, pp. 131f.

[13] J. Lepley, K. Brooks, and D. Bell, "A New Technology Electronic Ignition Which Eliminates the Limitations of Traditional Ignition Systems," Paper No. 173, CIMAC Congress 2010, Bergen.

[14] G. Meyer, S. Salbrechter, A. Tilz, and A. Wimmer, "Assessment of Electric Arc Models used in Recent Spark Ignition Models," in: "Digital Proceedings of the 8th European Combustion Meeting," Dubrovnik, 2017, pp. 644–648.

[15] D. Lepley and L. Tozzi, "Enhancing Spark-plug Life in Large Gas Engines," in: "MTZ industrial," vol. 6, no. 2, Jun. 2016, pp. 46–52.

[16] A. Schneider, P. Leick, A. Hettinger, and H. Rottengruber, "Experimental studies on spark stability in an optical combustion vessel under flowing conditions," in: Liebl, J.; Beidl, C. (Eds.): "Internationaler Motorenkongress 2016", 1st edition, Wiesbaden, 2016, pp. 327-348.

[17] G. S. Settles, „Schlieren and Shadowgraph Techniques: Visualizing Phenomena in Transparent Media," Berlin Heidelberg, 2001.

[18] M. Ninaus, "Anwendung der Ionenstrommessung zur Analyse des Verbrennungsablaufes bei direkteinspritzenden Dieselmotoren," Master Thesis, Graz University of Technology, Graz, 2003, pp. 78ff.

[19] H. Fabian, "Entwicklung eines Ionenstrommeßsystems für Verbrennungskraftmotoren," Master Thesis, Graz University of Technology, Graz, 1999, pp.115f.